Journal of Ideas in Health

e ISSN: 2645-9248 Journal homepage: www.jidhealth.com Open Access

Original Article

An automated approach for the kidney segmentation and detection of kidney stones on computed tomography using YOLO algorithms

Salman F. Rabby[1], Farhad Hossain[2], Shuvro C. Das[1], Imdadur Rahman[1], Srejon Das[1], Janibul A. Soeb[3], Md. Fahad Jubayer[4*]

Abstract

Background: For effective diagnosis and treatment planning, accurate segmentation of the kidneys and detection of kidney stones are crucial. Traditional procedures are time-consuming and subject to observer variation. This study proposes an automated method employing YOLO (You Only Look Once) algorithms for renal segmentation and kidney stone detection on CT scans to address these issues.

Methods: The dataset used in this study was sourced from the GitHub. The dataset contains a total of 1799 images, with 790 images labeled as 'containing kidney stones' and 1009 images labeled as 'not containing kidney stones'. U-Net architecture was utilized to precisely identify the region of interest, while YOLOv5 and YOLOv7 architecture was utilized to detect the stones. In addition, a performance comparison between the two YOLO models and other contemporary relevant models has been conducted.

Results: We obtained a kidney segmentation IOU (Intersection over Union) of 91.4% and kidney stone detection accuracies of 99.5% for YOLOv7 and 98.7% for YOLOv5. YOLOv5 and YOLOv7 outperform the best existing models, including CNN, KNN, SVM, Kronecker CNN, Xresnet50, VGG16, etc. YOLOv7 possesses superior accuracy than YOLOv5. The only issue we encountered with the YOLOv7 model was that it demanded more training time than the YOLOv5 model.

Conclusion: The results demonstrate that the proposed AI-based method has the potential to improve clinical procedures, allowing radiologists and urologists to make well-informed decisions for patients with renal pathologies. As medical imaging technology progresses, the incorporation of deep learning techniques such as YOLO holds promise for additional advances in automated diagnosis and treatment planning.

Keywords: Deep Learning, YOLOv7, YOLOv5, Medical Imaging, Kidney, Bangladesh

Background

The field of medical imaging has been significantly transformed by the advent of computed tomography (CT) [1]. Renal health assessment, specifically kidney segmentation and stone detection, has emerged as a crucial diagnostic tool within a wide range of applications. The precise and effective analysis of CT scans is of utmost importance in assisting healthcare practitioners in making informed decisions and delivering prompt interventions [2]. In recent years, there has been significant progress in object detection tasks across various domains through the utilization of deep learning-based algorithms, specifically, the You Only Look Once (YOLO) framework. YOLO is a single-stage detector, so it can detect all of the objects in an image with a single forward transit through a convolutional neural network (CNN). It utilizes a singular neural network to predict the bounding boxes and class probabilities of the objects present in an image, making YOLO extremely fast [3]. The incorporation of the YOLO in medical contexts holds promise for enhancing the precision and effectiveness of medical diagnoses. YOLO is particularly attractive for time-sensitive medical procedures and clinical decisions such as disease detection, treatment planning, and monitoring of disease progression due to its real-time performance [4]. Kidney segmentation plays a crucial role in facilitating disease diagnosis and enhancing treatment planning. Accurate segmentation of kidney structures yields valuable insights into irregularities pertaining to shape and size. These findings can be leveraged by medical professionals to analyze critical clinical conditions, such as carcinoma [5]. CT imaging

*Correspondence: fahadbau21@hotmail.com
[1]Department of Food Engineering and Technology, Sylhet Agricultural University, Sylhet-3100, Bangladesh
A full list of author information is available at the end of the article

is preferred by radiologists over other imaging techniques because it generates high-resolution images with clear anatomical details. Consequently, CT imaging is an indispensable diagnostic instrument for any disease affecting the kidneys [2]. Manual segmentation, despite being regarded as the gold standard, is labor-intensive, prone to human error, and time-consuming. Kidney stones are a prevalent medical condition with a global impact, leading a significant number of individuals to seek urgent medical attention due to severe discomfort [6]. Unless detected and treated early, it can develop and cause severe pain, as well as a high likelihood of obstructing the urinary system and causing kidney failure [7]. Even though there are numerous imaging techniques available, selecting the most appropriate one for kidney stone detection can vary from patient to patient. However, non-contrast computed tomography (NCCT) is considered the most accurate imaging technique due to its high sensitivity, specificity, and precise detection of the stone size [8]. Due to the unprecedented amount of computational power and advanced imaging techniques, we can meticulously analyze medical images and detect details that human eyes may have overlooked. Deep learning offers algorithms that are effective for image segmentation [9], object detection [10], and classification [11]. Deep learning is becoming increasingly valuable in urology for the detection of kidney stones [12]. Among the pertinent works is the early detection of chronic kidney disease using machine learning techniques [13]. Using deep learning techniques, a recent study has devised a computer-assisted diagnostic technique for detecting kidney stones in coronal CT scans. Baygin et al. introduced ExDark19, a transfer learning-based image classification method for automated kidney stone detection using CT images, in a separate study [14]. Nonetheless, there are rarely any studies that use YOLO algorithms for the automated segmentation and detection of kidney and kidney diseases. In our study, we developed a model that first segments the kidneys from the NCCT images using the U-Net architecture and then detects kidney stones with the YOLO algorithms. Due to the absence of any other organ in the image, segmenting the kidneys increases the efficacy of stone detection. The research questions for this article could include:

1. How can YOLO algorithms be adapted and implemented for automatic kidney segmentation and kidney stone detection in computed tomography (CT) images?
2. Can the YOLO-based system accurately differentiate kidney stones from other common kidney anomalies on CT scans?

We hypothesized that AI can be efficiently used to diagnose and detect kidney stones. Hence, this article aims to address the automatic segmentation of kidneys and kidney stones in NCCT images using YOLOv7 and YOLOv5 algorithms. The goal of this present study is to detect the stone as exactly as possible, which leads to image processing. The current study has the following contributions.

1. A cutting-edge automated approach for kidney segmentation and the detection of kidney stones on CT scans, leveraging the YOLO framework.
2. This novel method offers healthcare professionals a powerful tool to improve patient outcomes and streamline the diagnostic process.

As the prevalence of kidney-related disorders continues to rise, the findings of this study are anticipated to have a substantial impact on the field of medical imaging and deep learning applications in healthcare.

Methods

U-Net architecture was used to precisely determine the region of interest, while YOLOv5 and YOLOv7 architecture were used to detect the stones. Each utilizes convolutional neural networks. Figure 1 provides a comprehensive illustration of the workflow.

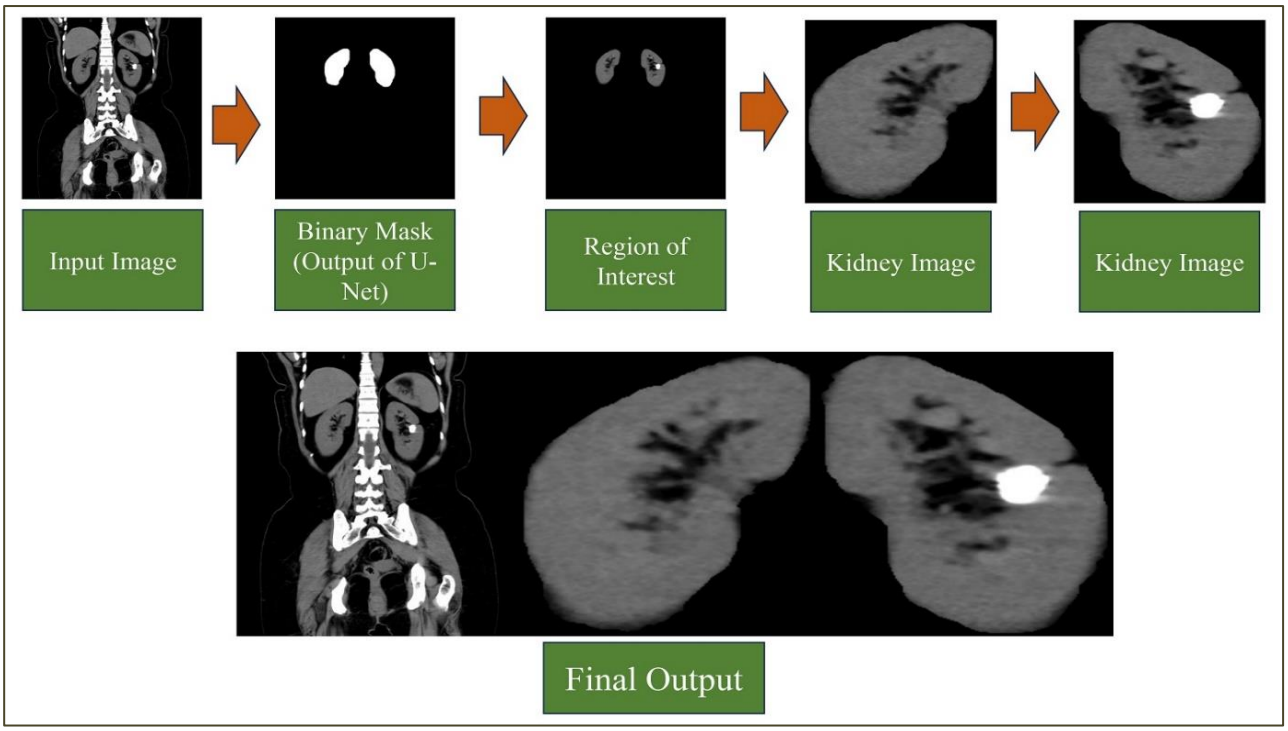

Figure 1. Workflow of the whole process of kidney segmentation and stone detection.

Dataset description

The dataset employed in this study was sourced from the kidney stone detection repository available on GitHub [12]. The repository comprises a varied collection of coronal CT scans obtained from multiple institutions and scanners. The scans within the dataset were obtained in the Digital Imaging and Communications in Medicine (DICOM) format and underwent pre-processing to eliminate any personal identification details pertaining to the patient. Without contrast administration, every image was captured in the supine position. The dataset comprises a total of 1799 images, with 790 images labeled by radiologists and urologists as containing kidney stones and 1009 images labeled as not containing kidney stones.

The dataset consists of CT scans from male and female patients spanning ages from 18 to 80 years. For testing, we categorized a total of 165 images as containing stones and 181 images as not containing stones. The remaining images were allocated for the tasks of creating binary masks, labeling, training, and validation. This database is made publicly available Yildirim et al. [12], at the following ink: (https://github.com/yildirimozal/Kidney_stone_detection). The distribution of data for training, validation, and testing for both U-Net and YOLO is shown in Figure 2.

Figure 3 depicts the NCCT images with and without kidney stones from the dataset used for training, validation, and testing.

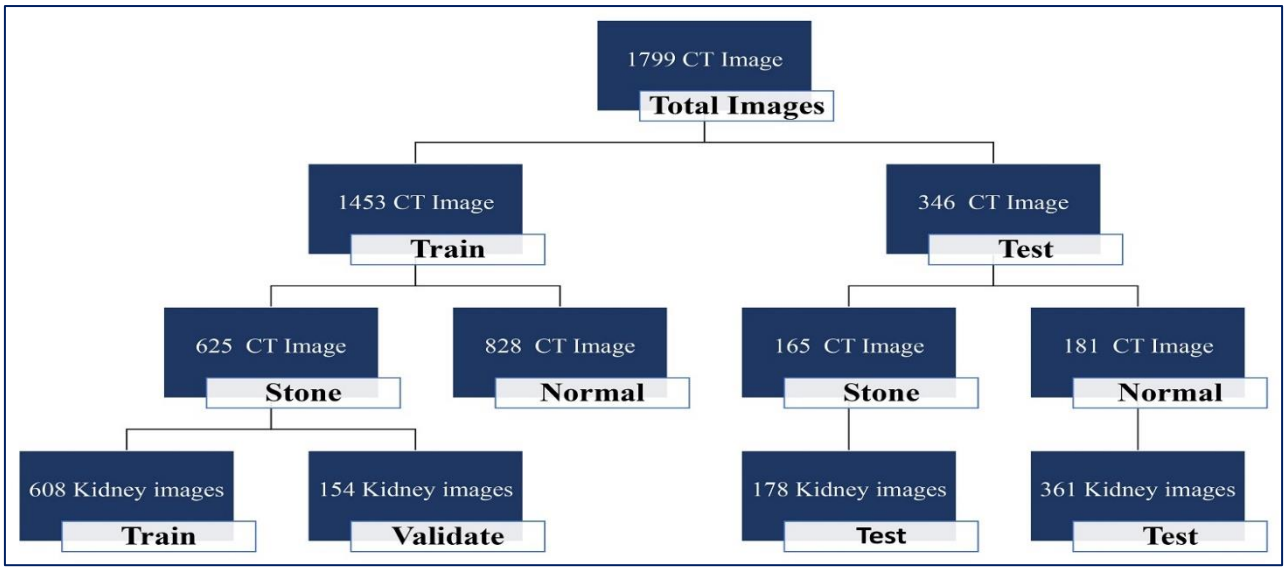

Figure 2. Data distribution for both U-Net and YOLO models

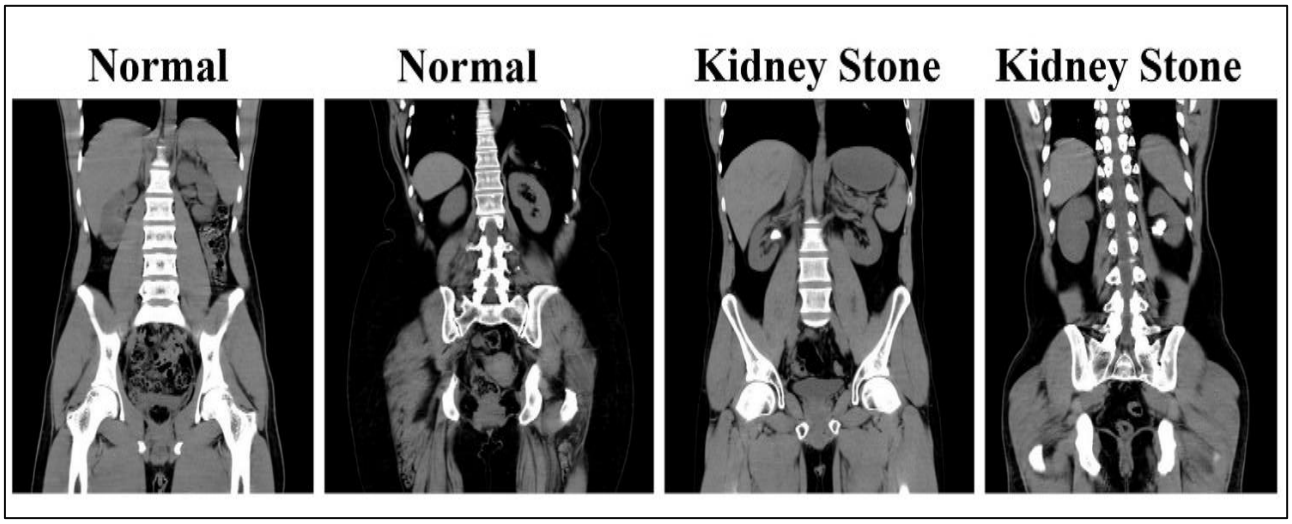

Figure 3: Typical examples of normal and kidney stone NCCT images are used in this study provided by Yildirim et al [12].

Data for U-Net

We gathered 1453 images for training and validation, with 80% devoted to training and 20% to validation. We used label-studio to create each image's mask. Every image had one left mask (for the left kidney) and one right mask (for the right kidney). The masks are then converted to binary masks containing only 0 and 255 as pixel values. The model took three folders as input, where the first folder contained all the images, and the rest contained the respective masks for each image. The images and masks consist same name and sequence. The model resized the images and masks into 512×512 and split the data into two portions for training and validation.

Data for YOLO

We created a second data set containing 608 training images and 154 validation images for stone detection. The images were obtained by multiplying the original images with their respective binary masks, and contour detection was utilized to

obtain images of each kidney. We resized every image to 640×640 before labeling. The kidney images were separated into two folders containing images with and without stones. We used makesense.ai to designate the images with an appropriate bounding box around the stones. We trained both YOLOv5 and YOLOv7 models with the same dataset. YOLO and U-Net models were tested with 346 images. None of these images was used for either training or validation.

U-Net Training

The U-Net consists of two major parts. The left part is known as the contracting part, constituted by the general convolutional process. The right part is the expansive part, constituted by transposed 2D convolutional layers [15]. Before training, every image was resized into 512×512. The contracting path consists of four layers, each consisting of repeated applications of convolutions followed by a rectified linear unit (Relu) and a max pooling operation reducing the size in half after each stage. The U-Net model is trained on Google colab using 50 epochs and took 5 hours to train with the Tesla T4 GPU. The Adam optimization algorithm, dice loss, and binary-cross-entropy loss were used to adjust the parameters of the U-Net model. The model predicts binary masks as output. To increase the IOU, we trained the U-Net model again with inceptionv3 as the backbone using the same condition and dataset. After multiplying the predicted mask with the original image, we get the desired images where only the kidney is present. Then by applying contour detection, we get two separate images of both kidneys. The U-Net architecture is shown in Figure 4.

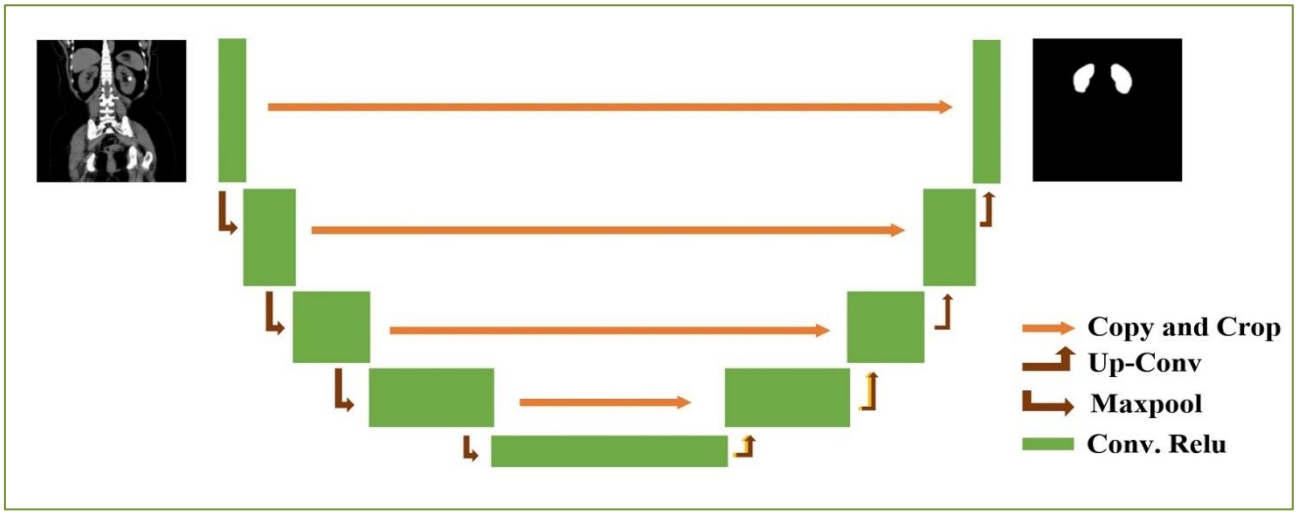

Figure 4: U-Net Architecture

YOLO Training

The YOLO network consists of 24 convolutional layers and two fully connected layers at the end. The convolutional layers extract the features of the image, and the fully connected layers predict the output coordinates and probabilities [16]. The bounding box contains five predictions: x, y, w, h, and confidence. We used 0.5 as the confidence threshold to predict the stones and only one class stone. We trained the YOLOv5 and YOLOv7 models on Google Colab using the Tesla T4 GPU with 100 epochs. The YOLO algorithm is quick and accurate, but the stones may be too small sometimes for it to detect efficiently. This problem is solved in YOLO versions 5 and 7. All the models are trained with the same dataset. The general procedure using YOLO models for this work is shown in Figure 5.

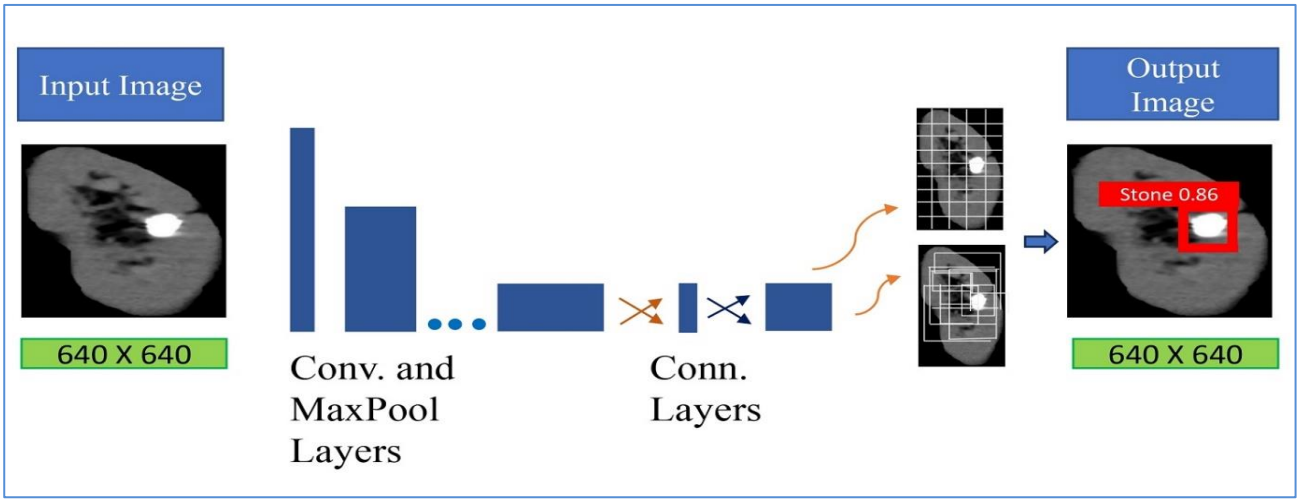

Figure 5: Process flow diagram of kidney stone detection using YOLO models

Results and discussion

Model performance

The split function randomly separated images for training and validation, and it took almost 5.5 hours to complete 50 epochs. We trained the U-Net model using the inceptionv3 as the backbone. The outcomes can be seen in Table 1. We evaluated the models using the 346 images we set aside. The model's accuracy is exceptionally high, as is typical for segmentation models. The IOU of the inceptionv3-trained U-Net model is 0.91. The IOU and dice coefficients indicate how near the prediction is to the actual value and the model's precision. (Table 1).

Table 1: Parameters obtained by U-Net models

Model-Name	IOU	F1 score	Validation loss
U-Net	0.72	0.83	0.15
U-Net with inception	0.91	0.95	0.04

The experimental findings encompassed four distinct outcomes: true positive (TP), false positive (FP), true negative (TN), and false negative (FN) [17]. However, it misclassified three kidney stone images as normal (FN) and five normal images as kidney stones (FP). Similarly, the YOLOv7 model accurately predicted 174 kidney stone images and 360 normal images. Nevertheless, it misclassified four kidney stone images and one normal image. Important statistical metrics are computed utilizing the following equations [17].

$$\text{Precision} = TP/(TP + FP) \quad (1)$$

$$\text{Recall} = TP/(TP + FN) \quad (2)$$

$$F1 - \text{score} = (2)/((1/\text{precision}) + (1/\text{recall})) \quad (3)$$

$$\text{Accuracy} = ((TP + TN / (TP + TN + FP + FN)) \quad (4)$$

The performance summary of the YOLO models can be observed in Table 2.

Table 2: Parameters obtained by the YOLO models

Model-Name	Precision	Recall	F1 Score	Accuracy
YOLOv5	0.98	0.97	0.98	0.98
YOLOv7	0.99	0.97	0.98	0.99

The confusion matrix depicted in Figures 6 (a) and 6 (b) compares the actual classification with the predicted classification. This phenomenon can serve as a visual representation of instances where the model experiences difficulty in accurately classifying or differentiating between two distinct classes. The representation is shown by a two-by-two matrix. One axis of the matrix corresponds to the real or ground truth, while the other axis corresponds to the truth as predicted by the model. According to the confusion matrix of the YOLOv5 model, 175 kidney stone (TP) images and 356 normal images (TN) were correctly predicted. While the YOLOv7 model's precise prediction for kidney stones is 174 images, it is 360 for normal images.

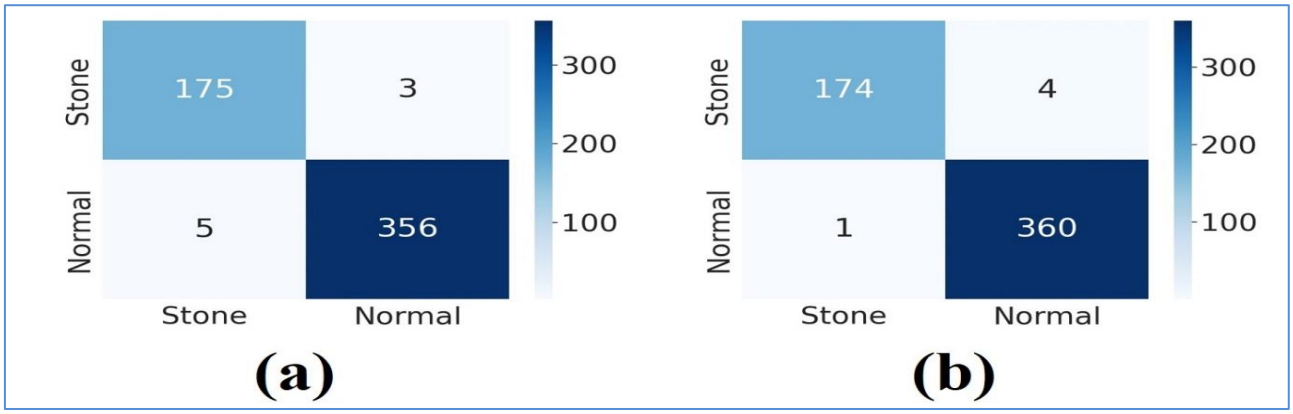

Figure 6: Confusion matrix diagram of (a) YOLOv5 and (b) YOLOv7.

Comparisons of U-Net and YOLO models

Using inceptionv3 improved the efficacy of the U-Net architecture, particularly the IOU and dice coefficient. Figure 7 demonstrates the difference. To detect kidney stones, YOLOv5 and YOLOv7 models were trained. Training the YOLOv7 model required less time than training the YOLOv5. Both models were trained on the same dataset and with the same number of epochs using the Tesla T4 GPU on Google Colab. With both models, we used a threshold value of 0.5 for detection. Figure 8 displays the comparison graphs. YOLOv7 has greater precision, while both models have the same recall value (Table 2). The YOLOv7 model has a more accurate prediction rate due to its increased precision. Both models predicted that four images containing a kidney stone were normal. Only one benign image was predicted to be a kidney stone by the YOLOv7 model. While YOLOv5 anticipated three. The YOLOv7 model incorrectly classified fewer images than the YOLOv5 model. The YOLOv7 model trained quicker and detected more accurately. The only difficulty we encountered with the YOLOv7 model was that it required longer training time than the YOLOv5 model. This result is consistent with a recent study by Soeb et al. [17]. The most accurate diagnosis is provided by NCCT images, which include the entire abdomen, pelvis, a portion of the thorax, and lower limbs. The kidneys are the region of interest, though they represent only a small portion of the total area. Therefore, it was imperative to precisely identify the area of interest [18]. The rib ends are nearly identical to larger kidney stones. Consequently, using the entire image for detection can result in less precise results. Due to the likelihood of detecting kidney stones in rib sites close to the kidneys. We segmented the kidneys using U-Net to reduce the likelihood of misidentification of other objects as kidney stones. normal image is detected as a kidney stone by both models, while a portion of the rib top is detected as a stone in two identical images (Figure 9).

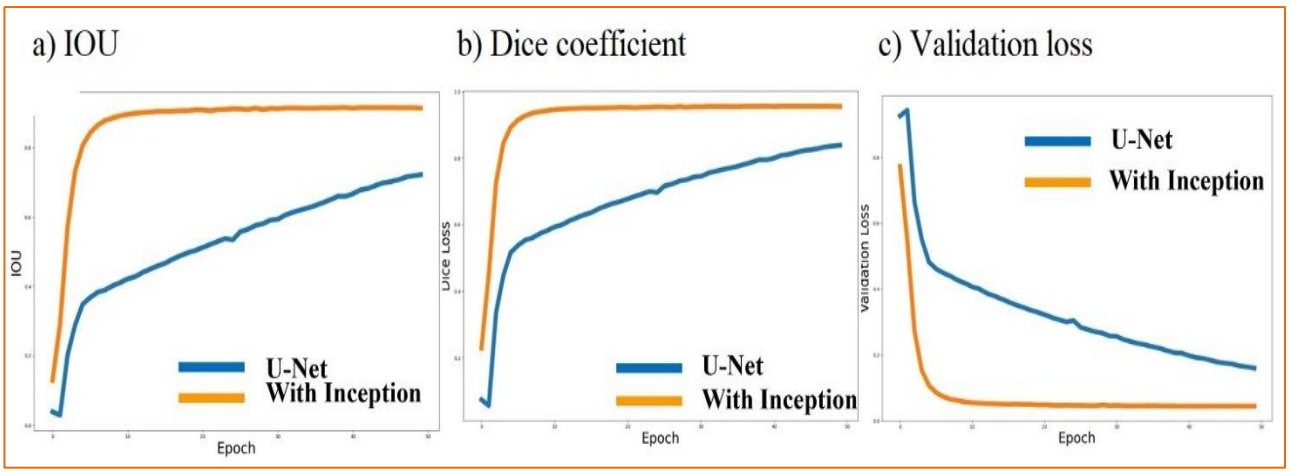

Figure 7: U-Net metrics comparison; a) IOU, b) dice coefficient, c) validation loss

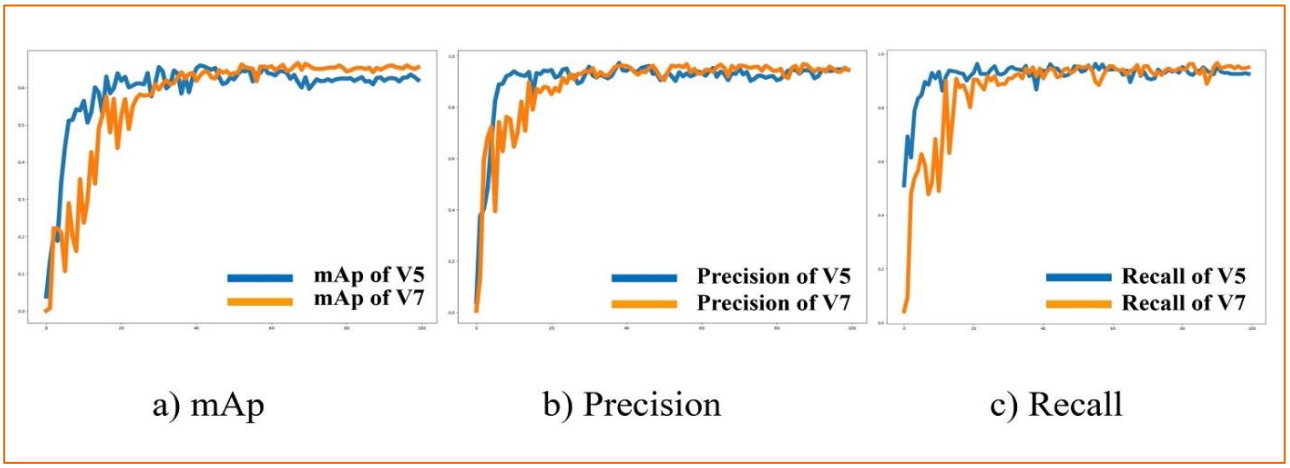

Figure 8: YOLO model metrics comparison; a) mAP, b) precision, c) recall

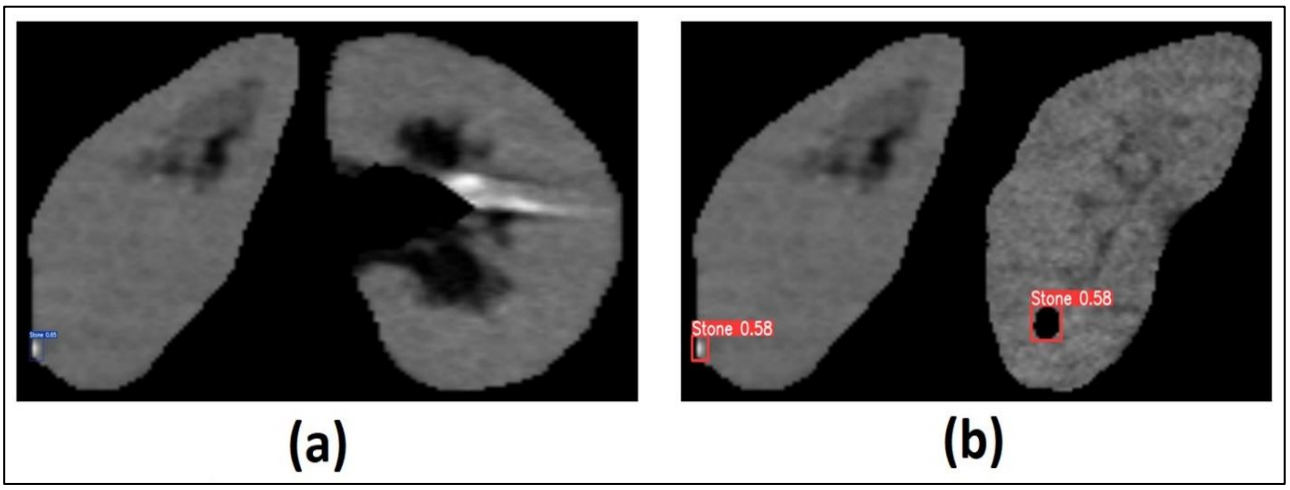

Figure 9: (a)YOLOv7 and (b) YOLOv5 fault images.

The efficacy of the proposed methodology for kidney stone detection is compared to that of previously published models. The outcomes are presented in Table 3. The table presents a comprehensive evaluation of the efficacy of different machine learning and deep learning models in the context of kidney segmentation and the identification of kidney stones in computed tomography imaging. The performance of the decision tree and SVM in kidney segmentation and stone detection is satisfactory. However, these models may lack the sophistication to capture complex patterns in CT scans when compared to more sophisticated models. Next, the K-Nearest Neighbors (KNN) algorithm, which is more data-driven than the previous models, outperformed them with an accuracy of 89.0%. This suggests that data-driven methods may be more

appropriate for this particular issue. Regarding deep learning models, the CNN's accuracy was 86%. This further supports the trend that data-driven, sophisticated models tend to perform better in image-related tasks. A more specialized version of CNN, the Kronecker CNN, substantially improved accuracy to 98.5%, indicating that customizations and refinements to standard CNNs can result in significant performance improvements. The YOLO models are explicitly designed for object detection tasks, and their accuracy rates are quite impressive. YOLOv7 is as accurate as VGG16, indicating that specialized models designed for specific tasks (such as YOLO for object detection) can match or even surpass the performance of general-purpose models such as VGG16. The models developed in this study, YOLOv5 and YOLOv7, outperform the best pre-existing models, suggesting that they could be valuable additions to the toolbox of methods for tackling this crucial medical task.

Table 3. Performance comparison of the current study with existing models

Model	Accuracy (%)	References
CNN	86.0	[19]
Decision tree	85.3	[20]
KNN	89.0	[21]
SVM	84.0	[21]
Kronecker CNN	98.5	[22]
Xresnet50	96.8	[12]
VGG16	99.0	[16]
YOLOv5	98.7	Present study
YOLOv7	99.5	Present study

When radiologists have to evaluate an increased volume of reports, they tend to accelerate the diagnostic process. Consequently, they may commit significant errors. There is evidence that 10% of radiologists missed important details when they screened a CT image for approximately 10 minutes, while the error rate increases to 26% when the screening duration is reduced by half [23]. Clinical radiology practice is associated with an error rate of approximately 4% [24]. If each image is evaluated by two expert radiologists, this error rate can be significantly reduced. However, this is not always feasible due to a lack of radiologists. Deep learning models can be used to perform the duties of a radiologist and generate a second opinion. Our proposed models are clinically reliable diagnostic tools due to their high accuracy, ability to precisely determine the region of interest, and ability to detect kidney stones with precision.

Conclusion

The model can be enhanced by integrating more sophisticated algorithms and images from other imaging modalities, such as X-ray, ultrasonography, MRI, and CT. Additionally, images obtained from various planes and hospitals should be used to improve the model's accuracy and provide more information about the stones' locations. In the present study, a deep-learning model was proposed for the automated detection of kidney stones using NCCT images. The model employs image segmentation to precisely distinguish the kidneys and detect kidney stones. To validate the performance of our model, we enlisted the assistance of a specialist Urologist from Sylhet MAG Osmani Medical College and Hospital, Bangladesh, who evaluated the results and determined that the regions of interest identified by our model were accurate for the majority of images. This suggests that our proposed model is accurate and can be utilized by radiologists as a dependable tool for detecting kidney stone cases rapidly and effectively.

Abbreviation

CT: Computed Tomography; YOLO: You Only Look Once; CNN: Convolutional Neural Network; NCCT: Non-Contrast Computed Tomography; IoU: Intersection over Union; DICOM: Digital Imaging and Communications in Medicine; TP: True Positive, FP: False Positive, TN: True Negative, FN: False Negative; KNN: K-Nearest Neighbors

Declaration

Acknowledgment

None.

Funding

The authors received no financial support for their research, authorship, and/or publication of this article.

Availability of data and materials

Data will be available by emailing fahadbau21@hotmail.com

Authors' contributions

Salman F. Rabby (SFR), and Janibul A. Soeb (JAB) were involved in conceptualization, writing original draft, and supervision; Farhad Hossain (FH) performed the data analysis, writing, reviewing and editing; Shuvro C. Das (SCD), Imdadur Rahman (IR), and Srejon Das (SD) were involved in programming, formal data analysis, writing original draft; Md. Fahad Jubayer (MFJ) conceptualized and supervised the research and engaged in writing original draft, reviewing and editing.

Ethics approval and consent to participate

We conducted the research following the declaration of Helsinki. The data used in this study was obtained from an open access repository (https://github.com/yildirimozal/Kidney_stone_detection), Provided by Yildirim et al. [12], Therefor there was no need for obtaining any ethical consent.

Consent for publication

Not applicable

Competing interest

The authors declare that they have no competing interests.

Author Details

[1]Department of Electrical and Electronic Engineering, Sylhet Engineering College, Sylhet, 3100, Bangladesh.
[2]Department of Health Management Information System, Mymensingh Medical College Hospital, Mymensingh-2200, Bangladesh.
[3]Department of Farm Power and Machinery, Sylhet Agricultural University, Sylhet-3100, Bangladesh.
[4]Department of Food Engineering and Technology, Sylhet Agricultural University, Sylhet-3100, Bangladesh.

Article Info
Received: 15 September 2023
Accepted: 02 November 2023
Published: 27 November 2023

References

1. Power SP, Moloney F, Twomey M, James K, O'Connor OJ, Maher MM. Computed tomography and patient risk: Facts, perceptions and uncertainties. World Journal of Radiology. 2016;8(12):902-15. https://doi.org/10.4329%2Fwjr.v8.i12.902
2. Caglayan A, Horsanali MO, Kocadurdu K, Ismailoglu E, Guneyli S. Deep learning model-assisted detection of kidney stones on computed tomography. International Braz J Urol. 2022; 48:830-9. https://doi.org/10.1590/S1677-5538.IBJU.2022.0132
3. Fang W, Wang L, Ren P. Tinier-YOLO: A real-time object detection method for constrained environments. IEEE Access. 2019; 8:1935-44. https://doi.org/10.1109/ACCESS.2019.2961959
4. Pacal I, Karaman A, Karaboga D, Akay B, Basturk A, Nalbantoglu U, Coskun S. An efficient real-time colonic polyp detection with YOLO algorithms trained by using negative samples and large datasets. Computers in Biology and Medicine. 2022; 141:105031. https://doi.org/10.1016/j.compbiomed.2021.105031
5. da Cruz LB, Araújo JD, Ferreira JL, Diniz JO, Silva AC, de Almeida JD, de Paiva AC, Gattass M. Kidney segmentation from computed tomography images using deep neural network. Computers in Biology and Medicine. 2020; 123:103906. https://doi.org/10.1016/j.compbiomed.2020.103906
6. Daudon M, Williams Jr JC. Characteristics of human kidney stones. Kidney Stones: Medical and Surgical Management. 2019; 30:77.
7. Singh P, Granberg CF, Harris PC, Lieske JC, Licht JH, Weiss A, Milliner DS. Primary hyperoxaluria type 3 can also result in kidney failure: a case report. American Journal of Kidney Diseases. 2022;79(1):125-8. https://doi.org/10.1053/j.ajkd.2021.05.016
8. Nestler T, Haneder S, Hokamp NG. Modern imaging techniques in urinary stone disease. Current Opinion in Urology. 2019;29(2):81-8.
9. Isensee F, Jaeger PF, Kohl SA, Petersen J, Maier-Hein KH. nnU-Net: a self-configuring method for deep learning-based biomedical image segmentation. Nature Methods. 2021;18(2):203-11. https://doi.org/10.1038/s41592-020-01008-z
10. Wu X, Sahoo D, Hoi SC. Recent advances in deep learning for object detection. Neurocomputing. 2020;396:39-64. https://doi.org/10.1016/j.neucom.2020.01.085
11. Zhang J, Xie Y, Wu Q, Xia Y. Medical image classification using synergic deep learning. Medical Image Analysis. 2019;54:10-9. https://doi.org/10.1016/j.media.2019.02.010
12. Yildirim K, Bozdag PG, Talo M, Yildirim O, Karabatak M, Acharya UR. Deep learning model for automated kidney stone detection using coronal CT images. Computers in Biology and Medicine. 2021;135:104569. https://doi.org/10.1016/j.compbiomed.2021.104569
13. Almansour NA, Syed HF, Khayat NR, Altheeb RK, Juri RE, Alhiyafi J, Alrashed S, Olatunji SO. Neural network and support vector machine for the prediction of chronic kidney disease: A comparative study. Computers in Biology and Medicine. 2019; 109:101-11. https://doi.org/10.1016/j.compbiomed.2019.04.017
14. Baygin M, Yaman O, Barua PD, Dogan S, Tuncer T, Acharya UR. Exemplar Darknet19 feature generation technique for automated kidney stone detection with coronal CT images. Artificial Intelligence in Medicine. 2022; 127:102274. https://doi.org/10.1016/j.artmed.2022.102274
15. Causey J, Stubblefield J, Qualls J, Fowler J, Cai L, Walker K, Guan Y, Huang X. An ensemble of u-net models for kidney tumor segmentation with CT images. IEEE/ACM Transactions on Computational Biology and Bioinformatics. 2021;19(3):1387-92. https://doi.org/10.1109/TCBB.2021.3085608
16. Jubayer F, Soeb JA, Mojumder AN, Paul MK, Barua P, Kayshar S, Akter SS, Rahman M, Islam A. Detection of mold on the food surface using YOLOv5. Current Research in Food Science. 2021; 4:724-8. https://doi.org/10.1016/j.crfs.2021.10.003
17. Soeb MJ, Jubayer MF, Tarin TA, Al Mamun MR, Ruhad FM, Parven A, Mubarak NM, Karri SL, Meftaul IM. Tea leaf disease detection and identification based on YOLOv7 (YOLO-T). Scientific Reports. 2023;13(1):6078. https://doi.org/10.1038/s41598-023-33270-4
18. Serrell EC, Best SL. Imaging in stone diagnosis and surgical planning. Current Opinion in Urology. 2022;32(4):397-404. https://doi.org/10.1097/MOU.0000000000001002
19. Apena WO, Joseph OL. Convolutional neural network model layers improvement for segmentation and classification on kidney stone images using keras and tensorflow. Journal of Multidisciplinary Engineering Science and Technology. 2021;8(6):14151-56
20. Aksakalli I, Kaçdioğlu S, Hanay Ys. Kidney x-ray images classification using machine learning and deep learning methods. Balkan Journal of Electrical and Computer Engineering. 2021;9(2):144-51. https://doi.org/10.17694/bajece.878116
21. Verma J, Nath M, Tripathi P, Saini KK. Analysis and identification of kidney stone using K th nearest neighbour (KNN) and support vector machine (SVM) classification techniques. Pattern Recognition and Image Analysis. 2017;27:574-80. https://doi.org/10.1134/S1054661817030294
22. Patro KK, Allam JP, Neelapu BC, Tadeusiewicz R, Acharya UR, Hammad M, Yildirim O, Pławiak P. Application of Kronecker convolutions in deep learning technique for automated detection of kidney stones with coronal CT images. Information Sciences. 2023;640:119005. https://doi.org/10.1016/j.ins.2023.119005
23. Akshaya M, Nithushaa R, Raja NS, Padmapriya S. Kidney stone detection using neural networks. In 2020 International Conference on System, Computation, Automation and Networking (ICSCAN) 2020 Jul 3 (pp. 1-4). IEEE. https://doi.org/10.1109/ICSCAN49426.2020.9262335
24. Vishmitha D, Yoshika K, Sivalakshmi P, Chowdary V, Shanthi KG, Yamini M. Kidney Stone Detection Using Deep Learning and Transfer Learning. In 2022 4th International Conference on Inventive Research in Computing Applications (ICIRCA) 2022 (pp. 987-992). IEEE. https://doi.org/10.1109/ICIRCA54612.2022.998572